Environ Earth Sci (2015) 73:1629–1640
DOI 10.1007/s12665-014-3513-1

ORIGINAL ARTICLE

Three-dimensional run-out analysis and prediction of flow-like landslides using smoothed particle hydrodynamics

Man Hu · M. B. Liu · M. W. Xie · G. R. Liu

Received: 12 July 2013 / Accepted: 2 July 2014 / Published online: 3 August 2014

Abstract Many landslides can often be characterized as a sort of landslides which move rapidly like flowing fluid and thus have a long run-out. They usually cause large damage and casualties especially when they are trigged by an earthquake or heavy rain. Numerical simulations of flow-like landslides are difficult due to the existence of free surface and large flow deformations. In this work, the smoothed particle hydrodynamics (SPH) method is applied to model two- and three-dimensional flow-like landslides for the run-out analysis. This is because SPH method is a meshfree, Lagrangian particle method, and is believed to be superior to conventional numerical methods in treating free surfaces, moving interfaces, and large deformations; hence, it is ideal in describing the complex fluidization characteristics in flow-like landslides. In this paper, a Bingham flow model and Navier–Stokes equations are incorporated into the SPH frame work, in which fluids are discretized by flow particles, and 3D terrain topography from GIS is represented by surface (or solid wall) particles. An improved SPH method is first applied to simulate the whole run-out processes of three flow-like landslides, which were triggered by Wenchuan earthquake that occurred in China in 2008. The effectiveness of the improved SPH method in modeling flow-like landslides is demonstrated by the good agreement of the 3D profile simulation results obtained from the present SPH simulation with field observation and results from other open sources. The SPH method is then used to predict the run-out area of Jinpingzi landslide.

Keywords Flow-like landslides · Run-out analysis · Smoothed particle hydrodynamics · Hazardous area prediction · Three-dimensional simulation

Introduction

The stability and run-out analysis of large landslides are usually important as they can cause tremendous damages and casualties. Investigation and prediction of landslides are, however, very difficult due to complex geological and weather conditions. Large and fast moving landslides often exhibit a complex behavior showing a continuum passing from sliding to flowing. According to the classification of landslides, there is a term “flow-like landslides” to describe these types of landslides with extremely fast speed. Flow-like landslides are a sort of landslides which move rapidly, have a longer run-out (from several 100 m up to several kilometers) than the other types of landslides, and also probably cause greater damages and casualties (Pastor et al. 2009; Huang et al. 2012; Cascini et al. 2014). Flow-like landslides are easily triggered by earthquakes and heavy rain fails. For example, in 2008, more than 1,500 flow-like landslides were

---

Electronic supplementary material The online version of this article (doi:10.1007/s12665-014-3513-1) contains supplementary material, which is available to authorized users.

M. Hu · M. W. Xie
School of Civil and Environmental Engineering, University of Science and Technology Beijing, Beijing 100083, China

M. Hu (✉) · G. R. Liu
Department of Aerospace Engineering and Engineering Mechanics, University of Cincinnati, Cincinnati, OH 45221-0070, USA
e-mail: humanyyyes@gmail.com

M. B. Liu
LHO, Institute of Mechanics, Chinese Academy of Sciences, Beijing 100190, China

caused by Wenchuan earthquake with a loss of almost 20,000 people (Huang et al. 2011; Yin et al. 2009; Dai et al. 2014). Therefore, the prediction of run-out distances and velocity through simulating the propagation stage of flow-like landslides can help to significantly reduce losses caused by these disasters and also provide necessary information or suggestions for the design of protective devices. Numerical models can simulate the flow behavior of flow-like landslides and can be applied into the investigations, analysis and predictions of landslides. Presently, most of the research methods of studying landslides are based on solid mechanics analysis methods, such as limit equilibrium and finite element method (Duncan 1996; Hammouri et al. 2008) and the fracture mechanics method (Scavia 1995; Eberhardt et al. 2004). These methods focus on slope stability analysis, strain and stress analysis, and some promising results have been obtained. However, these methods are not able to simulate the extremely large movement of the slip body, and cannot be used to predict the run-out area during the dynamic propagation stage of a landslide. For large-scale landslides with flow-like movement behavior, this is especially true.

With the improvement of computational methods, advanced numerical methods have been developed recently on the basis of computational fluid dynamics (CFD) (Uzuoka et al. 1998). CFD methods can provide rigorous and precise solutions that are suitable for modeling the complicated large movement of flow behavior of concerned materials. Among the recent advanced numerical methods, SPH is a meshfree, adaptive and Lagrangian method. It was introduced by Lucy (1977), Gingold and Monaghan (1977) for modeling astrophysical problems. Since its invention, SPH has been extensively studied and extended to different areas in engineering and science. SPH has some special advantages over the traditional grid-based numerical methods. The major difficulties of grid-based numerical methods are that they suffer from grid distortions, which lead to inaccuracies in the solution or to failure of the computation for a continuum. Hence, as a purely Lagrangian meshfree method in which particles carry field variables and move with the material velocity, SPH can handle the problems with free surface, extremely large deformation and crack propagation, like the propagation stage of a landslide, and is relatively easy to incorporate complex geometries. Therefore, SPH is more suitable to the simulation of flow-like landslides.

The biggest advantage of SPH for modeling flow-like landslides is that SPH can readily accommodate large deformations and the post-failure stage of a landslide in materials. Couples of preliminary applications of SPH to landslides have been performed and very encouraging results have been obtained. For example, Pastor et al. (2009) proposed a depth-integrated, coupled SPH model for flow-like landslides. This model was derived from the velocity–pressure version of the Biot–Zienkiewicz model, and then it was applied to back-analyze the propagation stage of some catastrophic flow-like slope movements. A depth-averaged model for the simulation of rapid landslide motion across complex terrain was introduced by McDougall (McDougall and Hungr 2004). Run-out analysis was performed by Huang et al. (2012) for flow-like landslides triggered by the Ms 8.0 Wenchuan earthquake that occurred on 12 May 2008 in Sichuan Province, China, and simulation results showed good agreement with characteristics of flow-like landslides observed in the field. These applications demonstrate that SPH method is able to capture the major fundamental dynamic behavior of flow-like landslides, define the overall hazardous areas, and estimate the intensity of the hazard (Huang and Dai 2014). Therefore, it can help to design possible protective measures. However, the traditional SPH method encounters the problem of low accuracy. Also, the accuracy of the conventional SPH method is closely related to the distribution of particles. Because of these problems, the numerical simulations of landslides using traditional SPH are limited and more detailed studies are required to fully unleash the fullest potential of SPH techniques. Moreover, existing works on SHP are mostly based on two-dimensional analysis, which can be quite different from practical applications.

In this paper, an improved SPH method was used to analyze the run-out of flow-like landslides of large scale. For the improved SPH method, two modified schemes for density approximation and kernel gradient correction were implemented. The coupled boundary condition was adopted in the SPH simulation. A 3D SPH procedure was adopted with a combination of a Bingham flow model and the Navier–Stokes equations. To initiate the SPH particles, a practical scheme was devised to generate particles that filled up the landslide area, ghost particles on the slide bed. The 3D SPH model of flow-like landslide was then built with the help of the GIS software. The simulation result was compared with a 2D SPH model and a comparison study was conducted between these two. Finally, the run-out prediction of Jinpingzi landslide, which is located in Sichuan province, China, was carried out. It was found that the 3D SPH model is capable of providing a means to understand the 3D overall dynamic behaviors of moving landslides at large scale. It can be an appropriate way to effectively simulate these kinds of landslides. As the further study in this field, the comparisons between computational simulation results and field collected data in 3D should be carried out and modified models should be proposed.

Theoretical base of SPH

Basic concepts of SPH

Smoothed particle hydrodynamics is a meshless method introduced by Lucy, Gingold and Monaghan (1977). Liu and Liu (2003) provided a textbook with a comprehensive description of the SPH method from basic concept to engineering applications in different areas. Intensive efforts have been made by many researchers to extend the method to solve problems involving fluid flows and even solid mechanics. SPH has also been applied to model the propagation of catastrophic landslides (Hadush et al. 2000). SPH method is suitable for stimulating a class of flow-like landslides of extremely large movements, because it is a meshfree particle method without the limitation of mesh distortion in carrying out the flow issue. Also compared to Eulerian description it uses a Lagrangian description, which performs well in the problem of complex geometry, such as a natural landslide with irregular terrain data.

In the SPH method, the entire domain is discretized by a finite number of particles that carry individual mass and occupy individual space (Liu and Liu 2003). The Navier–Stokes equations are then discretized using these particles, and hence no mesh is needed afterwards. There are two key steps in the formulation of SPH. The first is the integral representation of filed functions, and the second is the particle approximation. Using the smoothing technique, the integral representation of function $f(x)$ can be formulated as following kernel approximation:

$$f(\boldsymbol{x}) = \int_{\Omega} f(\boldsymbol{x}')W(x-\boldsymbol{x}',h)\mathrm{d}\boldsymbol{x}' \tag{1}$$

where f is a field function related to the three-dimensional position vector $\boldsymbol{x}$, and $W(\boldsymbol{x}-\boldsymbol{x}',h)$ is the smoothing function. The integral representation of the derivative of function $f(\boldsymbol{x})$ can then be formulated as:

$$\nabla\cdot f(\boldsymbol{x}) = \int_{\mathrm{S}} f(\boldsymbol{x}')W(\boldsymbol{x}-\boldsymbol{x}',h)\cdot\vec{n}\mathrm{d}S - \int_{\Omega} f(\boldsymbol{x})\cdot\nabla W(\boldsymbol{x} - \boldsymbol{x}',h)\mathrm{d}\boldsymbol{x}' \tag{2}$$

For the particle approximation, since the whole domain has been discretized by particles, the continuous integration of kernel approximation of a field function at a particle can be obtained simply through summations over all particles within the support domain of the particle, as shown in Supplementary figure 1.

After some trivial transformation, Eqs. (1) and (2) can be rewritten as:

$$f(\boldsymbol{x}_i) = \sum\nolimits_{j=1}^{N}\frac{m_j}{\rho_j}f(\boldsymbol{x}_j)\cdot W_{ij} \tag{3}$$

$$\nabla\cdot f(\boldsymbol{x}_i) = -\sum\nolimits_{j=1}^{N}\frac{m_j}{\rho_j}f(\boldsymbol{x}_j)\cdot W_{ij} \tag{4}$$

For hydrodynamics of fluids described in Lagrangian formulation, the Navier–Stokes equations can be expressed as follows (Liu and Liu 2003):

$$\begin{cases} \rho_i = \sum\limits_{j=1}^{N} m_j W_{ij} \\ \dfrac{\mathrm{d}\boldsymbol{v}_i^{\alpha}}{\mathrm{d}t} = \sum\limits_{j=1}^{N} m_j \dfrac{\sigma_i^{\alpha\beta}+\sigma_j^{\alpha\beta}}{\rho_i\rho_j}\dfrac{\partial W_{ij}}{\partial \boldsymbol{x}_i^{\beta}} \\ \dfrac{\mathrm{d}e_i}{\mathrm{d}t} = \dfrac{1}{2}\sum\limits_{j=1}^{N} m_j\left(\dfrac{p_i}{\rho_i^2}+\dfrac{p_j}{\rho_j^2}\right)\boldsymbol{v}_{ij}^{\beta}\dfrac{\partial W_{ij}}{\partial \boldsymbol{x}_i^{\beta}} + \dfrac{\mu_i}{2\rho_i}\varepsilon_i^{\alpha\beta}\varepsilon_j^{\alpha\beta} \\ \dfrac{\mathrm{d}\boldsymbol{x}_i^{\alpha}}{\mathrm{d}t} = \boldsymbol{v}_i^{\alpha} \end{cases} \tag{5}$$

where ρ is scalar density, e is internal energy, $\boldsymbol{v}^{\alpha}$ is velocity component, and $\sigma^{\alpha\beta}$ is the total stress tensor, which are all dependent variables. $\boldsymbol{x}^{\alpha}$ is spatial coordinate and t is time, which are independent variables. The total stress tensor $\sigma^{\alpha\beta}$ in Eq. (5) is made up of two parts, one is isotropic pressure p and the other is shear stress $\tau^{\alpha\beta}$, where $\varepsilon^{\alpha\beta}$ is strain rate tensor.

Improved SPH method

As we know, the conventional SPH method has the problem of low accuracy as it cannot exactly reproduce quadratic and linear functions. Also, the accuracy of the conventional SPH method is closely related to the distribution of particles, selection of smoothing function and the support domain. During the past decade, many different attempts have been made and approaches have been proposed to improve the accuracy of SPH approximation (Chen and Beraun 2000; Liu et al. 2005; Liu and Liu 2006). In this paper, two modified schemes for approximating density (density correction) and kernel gradient (kernel gradient correction, or KGC) are adopted, which have been proved helpful to improve computational accuracy for modeling viscous impressible flows with changing and free surfaces (Shao et al. 2012). For the density correction, the density can be approximated as

$$\rho_{\mathrm{i}}^{\mathrm{new}} = \sum_{j=1}^{\mathrm{N}}\rho_{\mathrm{j}}W_{ij}^{\mathrm{new}}\frac{m_j}{\rho_j} = \sum_{j=1}^{\mathrm{N}} m_j W_{ij}^{\mathrm{new}} \tag{6}$$

$$W_{ij}^{\mathrm{new}} = \frac{W_{ij}}{\sum_{j=1}^{\mathrm{N}} W_{ij}\cdot\frac{m_j}{\rho_j}} \tag{7}$$

As to kernel gradient correction, based on Taylor series expansion on the SPH approximation of a function, the following formulation can be obtained.

$$\int_{\Omega} f(r')\nabla W \mathrm{d}r' = f(r)\int_{\Omega} \nabla W \mathrm{d}r' + \frac{\partial f(r)}{\partial x}\int_{\Omega} (x'-x)\nabla W \mathrm{d}r' + \frac{\partial f(r)}{\partial y}\int_{\Omega} \left(y'-y\right)\nabla W \mathrm{d}r' + \frac{\partial f(r)}{\partial z}\int_{\Omega} (z'-z)\nabla W \mathrm{d}r' + O\left(h^2\right) \tag{8}$$

Finally, after various transformations, it is can be further written as follows in terms of particle approximation.

$$\nabla f(r_i) = \frac{\partial f(r_i)}{\partial x_i}\sum_j (x_j - x_i)\nabla_i W_{ij} V_j + \frac{\partial f(r_i)}{\partial y_i}\sum_j (y_j - y_i)\nabla_i W_{ij} V_j + \frac{\partial f(r_i)}{\partial z_i}\sum_j (z_j - z_i)\nabla_i W_{ij} V_j + O\left(h^2\right) \tag{9}$$

where $V_j(= m_j/\rho_j)$ is the volume of particle j. From Eq. (9), it can be concluded that if $X = \begin{pmatrix} 1 \\ 0 \\ 0 \end{pmatrix}, Y = \begin{pmatrix} 0 \\ 1 \\ 0 \end{pmatrix}$ and $Z = \begin{pmatrix} 0 \\ 0 \\ 1 \end{pmatrix}$. The SPH particle approximation scheme for a gradient is of second-order accuracy. However, these three requirements cannot be satisfied in general cases. Therefore, it is possible to restore the accuracy with the following correction on the kernel gradient.

$$\nabla_i^{\mathrm{new}} W_{ij} = L(r_i)\nabla_i W_{ij} \tag{10}$$

$$L(r_i) = \left[\sum_j \begin{bmatrix} x_{ji}\frac{\partial W_{ij}}{\partial x_i} & y_{ji}\frac{\partial W_{ij}}{\partial x_i} & z_{ji}\frac{\partial W_{ij}}{\partial x_i} \\ x_{ji}\frac{\partial W_{ij}}{\partial y_i} & y_{ji}\frac{\partial W_{ij}}{\partial y_i} & z_{ji}\frac{\partial W_{ij}}{\partial y_i} \\ x_{ji}\frac{\partial W_{ij}}{\partial z_i} & y_{ji}\frac{\partial W_{ij}}{\partial z_i} & z_{ji}\frac{\partial W_{ij}}{\partial z_i} \end{bmatrix} V_j\right]^{-1} \tag{11}$$

It is noted that for both density correction and gradient correction, since only kernel and its gradient are corrected, there is no need to change the structure of SPH computer programs and procedure of SPH simulations. It is therefore convenient to implement SPH equations of motion.

Boundary treatment

One major challenge in SPH simulation is the boundary treatment, which has been influencing the accuracy of SPH. In this work, a coupled dynamic boundary treatment algorithm was adopted. In this method, two types of virtual particles, repulsive particles and ghost particles (as shown in Fig. 1), are used to represent the boundary. The repulsive particles produce a suitable repulsive force to the approaching real particles near the boundary, and they are located right on the solid boundary. Ghost particles are located outside the boundary area. In this approach, at the first time step the algorithm can generate ghost particles in a regular or irregular distribution, like landslide boundary, and the ghost particle positions do not need to change during following steps. More details can be found in the original work by Liu et al. (2012).

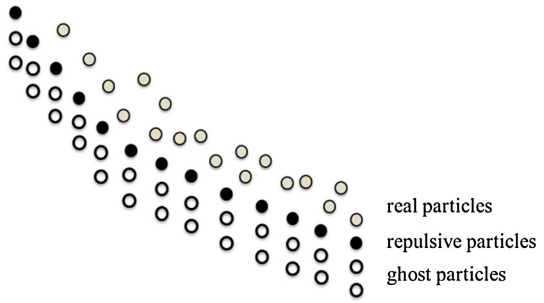

Fig. 1 Illustration of the coupled boundary condition algorithm

The algorithm for boundary treatment consists of two parts: a repulsive force and a new numerical scheme to approximate the information of the virtual particles. The repulsive force

$$\boldsymbol{F}_{ij} = 0.01c^2 \cdot \chi \cdot f(\eta) \cdot \frac{x_{ij}}{r_{ij}^2} \tag{12}$$

$$\eta = r_{ij}/(0.75h_{ij}), \quad \chi = 1 - r_{ij}/\Delta d, \quad 0 < r_{ij} < \Delta d$$

$$f(\eta) = \begin{cases} \frac{2}{3} & 0 < \eta \leq \frac{2}{3} \\ 2\eta - 1.5\eta^2 & \frac{2}{3} < \eta \leq 1 \\ 0.5(2-\eta)^2 & 1 < \eta < 2 \\ 0 & \text{otherwise} \end{cases} \tag{13}$$

where r is the distance between two particles and Δd is the initial distance of two adjacent particles. The soft repulsive force can prevent unphysical particle penetration without obvious pressure disturbances, which is different from the traditional repulsive boundary treatment algorithms with highly repulsive forces, such as the Lennard–Jones molecular force (Liu and Liu 2003). Besides, it is known that the support domains of the real particles intersect the boundary area with insufficient neighbor particles. Therefore, SPH particle approximation schemes with higher order accuracy can be used to improve the accuracy of boundary treatment, such as the Shepard filter method, moving least square (MLS) method, CSPM and FPM. In this study, the non-slip boundary condition (Morris et al. 1997) is used here. It has been demonstrated that the SPH particle approximations with higher order accuracy can lead to much better results than conventional SPH particle approximation schemes (Colagrossi and Landrini 2003). The variables of boundary particles (both repulsive and ghost particles) can be obtained as follows:

$$\rho_i^B = \sum_{j=1}^{N} \rho_j W_{ij}^{\text{new}} \frac{m_j}{\rho_j} = \sum_{j=1}^{N} m_j W_{ij}^{\text{new}} \tag{14}$$

$$v_i^B = -\sum_{j=1}^{N} v_i W_{ij}^{\text{new}} \frac{m_j}{\rho_j} \tag{15}$$

Constitutive model

The flow of many types of soils can often be described by the following constitutive equation:

$$\tau = \eta \dot{\gamma}^n + \tau_y \tag{16}$$

where τ is the shear stress, η is the viscosity, $\dot{\gamma}$ is the shear strain rate, and τ_y is the yield stress. Using different material parameters (η_0, n, τ_y), Eq. (16) is capable of describing the behavior of basic types of fluids, such as the Newtonian fluid, Bingham fluid, Pseudo plastic fluid, Dilatant fluid and ideal fluid, as shown in Supplementary figure 2. Among these five types of fluid model, the Newtonian fluid can be described by the well-known equation $\tau = \eta_0 \dot{\gamma}$. As one type of non-Newtonian fluid flows, Bingham flow can appropriately describe the relationship between shear strain rate and shear stress in highly deformed soil materials according to the research by Hadush et al. (2000). In this paper, the Bingham flow model is employed as the constitutive model in describing the fluidization characteristics of flow-like landslides, because it describes well many types of "flowing" soils (Huang et al. 2012; Hadush et al. 2000).

In the simulation, as the soil and water are treated as one single mixed component rather than two components differently, the ratio of water and soil can be important as it is closely related to the material models (constitutive model and equation of state). If the fraction of water is very high, mixture approaches water, and the landslide process is close to dam collapse problem. In contrast, if the fraction of soil is very high, the material model of solid should be used, and the landslide is triggered once the accumulated stress is sufficient to exceed the friction force in solid. This process involves a latent stage in accumulating stress, a starting process and flow-like fast moving stage. If the ratio of water and soil is medium, the mixture can be treated as some kind of non-Newtonian fluids as discussed in this paper.

For the Bingham fluid model, Eq. (16) can be expressed in the following form:

$$\tau = \eta \dot{\gamma}^n + \tau_y \tag{17}$$

where τ_y is the yield strength. Usually, Mohr–Coulomb yield criterion is used to describe the deformation characteristics of soil in soil Mechanics.

$$\tau = c + p\tan\varphi \tag{18}$$

Combined with the Mohr–Coulomb yield criterion, Eq. (17) can be transformed to:

$$\tau = \eta \dot{\gamma} + c + p\tan\varphi \tag{19}$$

where c is the cohesion, p is the pressure, and φ is the frictional angle.

An equivalent Newtonian viscosity is proposed to build a relationship between Bingham flow model and Newtonian flow model by Uzuoka et al. (1998). The equivalent Newtonian viscosity is described as:

$$\eta' = \eta + (c + p\tan\varphi)/\dot{\gamma} \tag{20}$$

The shear strain rate is calculated from:

$$\dot{\gamma} = \sqrt{\frac{\dot{e}_{ij}\dot{e}_{ij}}{2}} \tag{21}$$

In Eq. (20), an infinite equivalent viscosity coefficient arises when the shear strain rate equals zero. In order to overcome the problem, the maximum for equivalent viscosity can be determined by:

$$\begin{cases} \eta' = \eta_0 + \dfrac{\tau_y}{\dot{\gamma}} & (\eta' < \eta_m) \\ \eta' = \eta_m & (\eta' \geq \eta_m) \end{cases} \tag{22}$$

where η_{m} is the maximum of the equivalent viscosity coefficient. According to basic principles presented above, a SPH procedure and code are established based on the SPH code written in Visual Fortran (Liu and Liu 2003).

The verification of the SPH model mentioned above has been done with two classical benchmark problems, dam break and granular flow, which can be found in many research papers (Huang et al. 2012; Shao and Edmond 2003). The results agree with the test results. The accuracy of the SPH model has been verified and validated for these benchmarking problems. This study primarily focuses on the method of creating 3D SPH model, and then demonstrating its capability in simulating 3D fluidized large movements of landslides at large scale.

Scheme to generate particles of 3D SPH model

As a meshfree method, SPH does not need a mesh or grid as the computational frame. Particles are used to represent the concerned materials and to approximate the governing equations. In modeling flow-like landslides, fluids are discretized by flow particles, and 3D terrain topography from Geographical Information System (GIS) is represented by surface (or solid wall) particles. In another word, the real slope terrain topography usually can be expressed by Digital Elevation Models (DEMs) that are reliable and easily accessible. In GIS, DEMs are represented by grid/raster data which contain the elevation information. Then the particles, regularly distributing in slope area with

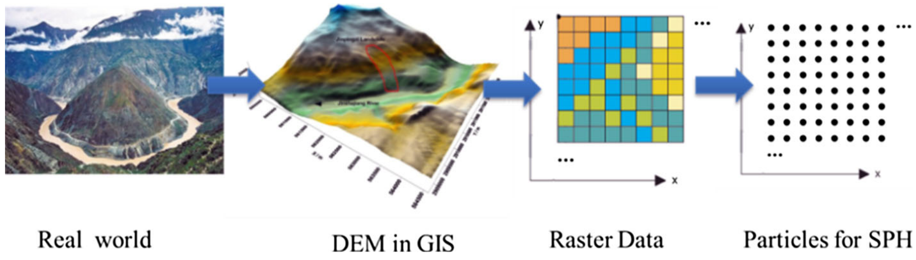

Fig. 2 The procedure of generating particles based on GIS

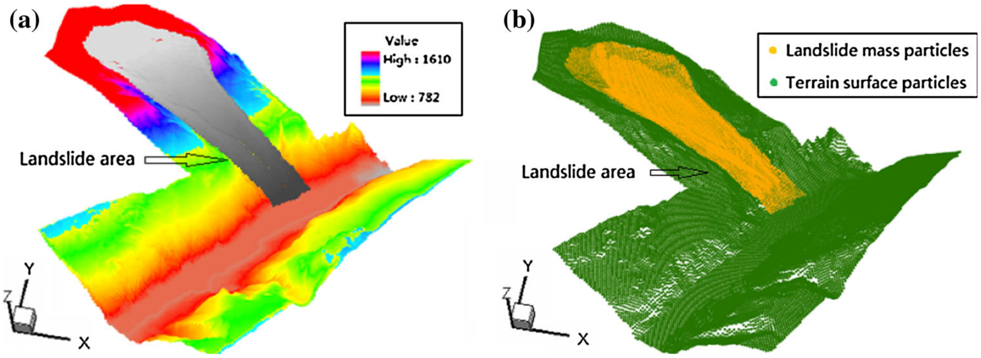

Fig. 3 Generating particles for 3D SPH models. **a** DEM for terrain surface and slip surface on the GIS platform; **b** landslide mass particles, slip surface and terrain surface particles

elevation information, can be extracted by use of GIS tools. Figure 2 shows the procedure of generating particles. The detailed scheme to generate the particles can be described as follow.

For 3D profile model, first the particles fitting to the topography in 2D plane are created. Two lines are derived from the pre-failure and post-failure topographies which could be compared with the SPH simulations. Before the generation of particles, one pre-failure topography line and one slip face line can be extracted from field collected data. Along the two lines which represent the pre-failure and the slip face line topographies, couples of points (or particles) can be placed with a certain interval on the basis of the GIS platform. In the case of Wangjiayan landslide, through the tool of editing topography of the software ArcMap, the vector points were inserted along the pre-failure topographies line and the slip face line with an interval of 10 m. Then particles can be interpolated into a pair of points which are in the same X coordinate with the certain interval through the interpolation of Matlab. After that, particles can be generated to fulfill the slip mass in the 2D profile plane with the same given interval. Finally, the 2D model was extended to 3D model in the Y coordinate which can create output data for all particles.

For 3D model of hazardous zone analysis, the particles were generated using the ArcMap and a program which was developed in Visual C#. DEMs were first created according to the terrain data of the landslide (like a contour map) in ArcMap. Three kinds of DEMs are needed to be created, the landslide mass terrain DEMs of landslide area, the slip face DEMs of landslide area, and the terrain DEMs of the whole surrounding mountain and valley area. Secondly, the slip face DEMs of landslide area and the terrain DEMs of the whole surrounding mountain and valley area should be merged to form a “sliding path” for the sliding mass. By the means of the ArcGIS tools which can convert grids to feature points, the “sliding path” raster was transformed to the ghost particles, and the ghost particle boundary was enhanced by staggering ghost particles in three layers. Each feature particle was placed in the center of each grid. The landslide mass terrain DEMs of landslide area and the slip face DEMs of landslide area were also transformed to particles. Each particle on the upper layer (which was made from landslide mass terrain DEMs of the landslide area) had the same X and Y coordinates as those on the lower layer particles (which were made from the slip face DEMs of the landslide area). Using these two upper and lower layers of particle, the interpolations in the Z direction were performed and all the particles were generated to fill up the entire volume. Figure 3a, b shows the DEMs of Jinpingzi landslide and the particles which were converted from the grid terrain surface and slip surface, respectively. The main principle used here is the equidistant interpolation between landslide mass terrain particles of landslide area and slip face particles. Due to the ability in processing geo-data of GIS, the complicated and irregular terrain can be expressed in reasonably good detail. In these cases, the interval between two closest particles is set at 10 m, in both horizontal and vertical directions.

Application and comparison of 3D SPH modeling to flow-like landslides in Wenchuan earthquake

In 2008, thousands of landslides and many other large-scale geological hazards were triggered by the Wenchuan earthquake in Sichuan Province, southwest of China. There are three large typical flow-like landslides, the Tangjiashan, Wangjiayan, and Donghekou landslides, which were among the most catastrophic, destroying many buildings and causing numerous casualties (Huang and Li 2009). The run-out analyses of these landslides were performed with 2D SPH models as applications of SPH modeling to real flow-like landslides by Huang et al. (2012). The result indicated that the fundamental dynamic behavior of flow-like landslides showed good agreements with site observations. In this paper, the 3D profile SPH models were built based on the 2D profile data. The deformation and failure process of these landslides were simulated.

Tangjiashan landslide

Tangjiashan landslide is located on the right bank of the Tongkou River. The large landslide killed 84 people in Wenchuan earthquake. The Tangjiashan landslide (Supplementary figure 3) had a height of 650 m and a horizontal sliding distance 900 m (Hu et al. 2009). It formed an extremely large impounded lake with a capacity of 250 million m^3.

A 2D SPH simulation of the Tangjiashan landslide was conducted to study by Huang et al. (2012). The 3D profile particle model was built to simulate the Tangjiashan landslide movement according to the 2D profile topographies data. Supplementary figure 4 is the 3D view of the SPH particle model captured in some moment of the moving process. The parameters used in the run-out analysis were derived from Hu et al. and Huang et al. The parameters are shown in Table 1. Figure 4 presents the simulated run-out process of the landslide and the topography evolution of the slip mass during its sliding.

A comparison of 2D SPH simulated geometry and landslide configuration (Huang et al. 2012) and the comparison between 2D profile SPH simulation and 3D profile SPH simulation are shown in Fig. 5 to demonstrate the quality of 3D SPH analysis.

Wangjiayan landslide

Wangjiayan landslide, one of the most destructive landslides during the Wenchuan earthquake, was a typical high-

Table 1 Parameters in the run-out analysis of the Tangjiashan landslide (Huang et al. 2012)

Density	ρ (kg/m^3)	2,000
Equivalent viscosity coefficient	η (Pa s)	1.9
Cohesion	c (kPa)	30
Angle of internal friction	φ (°)	30.0

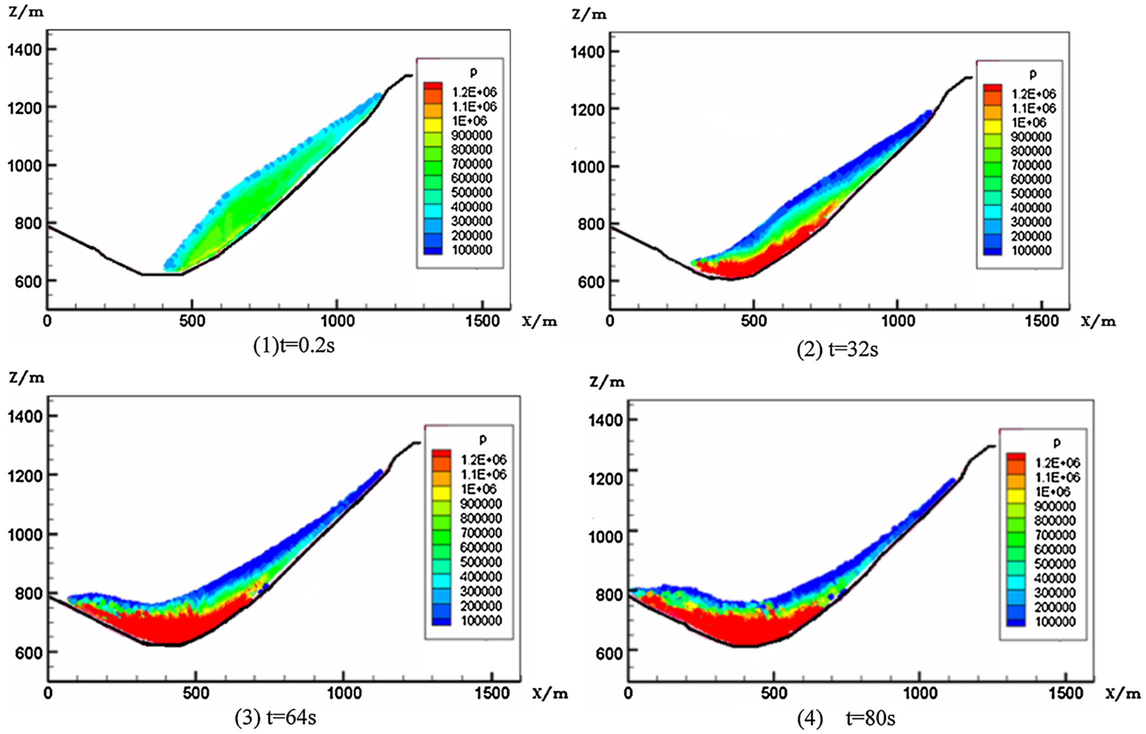

(1)t=0.2s (2) t=32s

(3) t=64s (4) t=80s

Fig. 4 Simulated run-out process of Tangjiashan landslide by 3D SPH model speed and long run-out landslide. It killed 1,600 people and destroyed hundreds of houses (Supplementary figure 5). The height difference between the front edge and back edge is 350 m, with a sliding distance of 550 m (Yin et al. 2009).

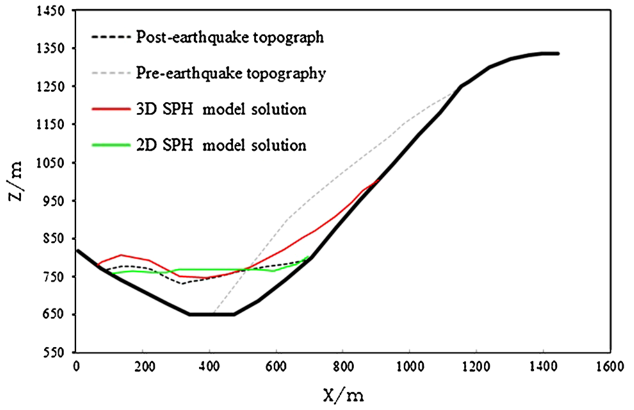

Fig. 5 Pre- and post-earthquake topographies, comparison of 2D and 3D SPH model for Tangjiashan landslide (Huang et al. 2012)

Table 2 Parameters in the run-out analysis of the Wangjiayan landslide (Huang et al. 2012)

Density	ρ (kg/m^3)	2,000
Equivalent viscosity coefficient	η (Pa s)	1.9
Cohesion	c (kPa)	30
Angle of internal friction	φ (°)	30.0

A 3D profile particle model was built to simulate the Wangjiayan landslide movement according to the 2D profile topographies data. Supplementary figure 6 is the 3D view of the SPH particle model captured in some moment of the moving process. The parameters which are derived from local engineering practice are shown in Table 2. Figure 6 presents the simulated run-out process of the Wangjiayan landslide by 3D SPH model.

A comparison of 2D SPH simulated geometry and landslide configuration (Huang et al. 2012) and the comparison between 2D profile SPH simulation and 3D profile SPH simulation are shown in Fig. 7 in order to check the quality of 3D SPH analysis.

Donghekou landslide

The Donghekou landslide which killed at least 300 people was extremely rapid and had a long run-out (Yin et al. 2009). The Donghekou landslide has a sliding distance of 2,400 m and a volume of 10 million m^3 (Sun et al. 2009) (Supplementary figure 7).

The 3D profile particle model was built to simulate the Donghekou landslide movement according to the 2D profile topographies data. Supplementary figure 8 is the 3D

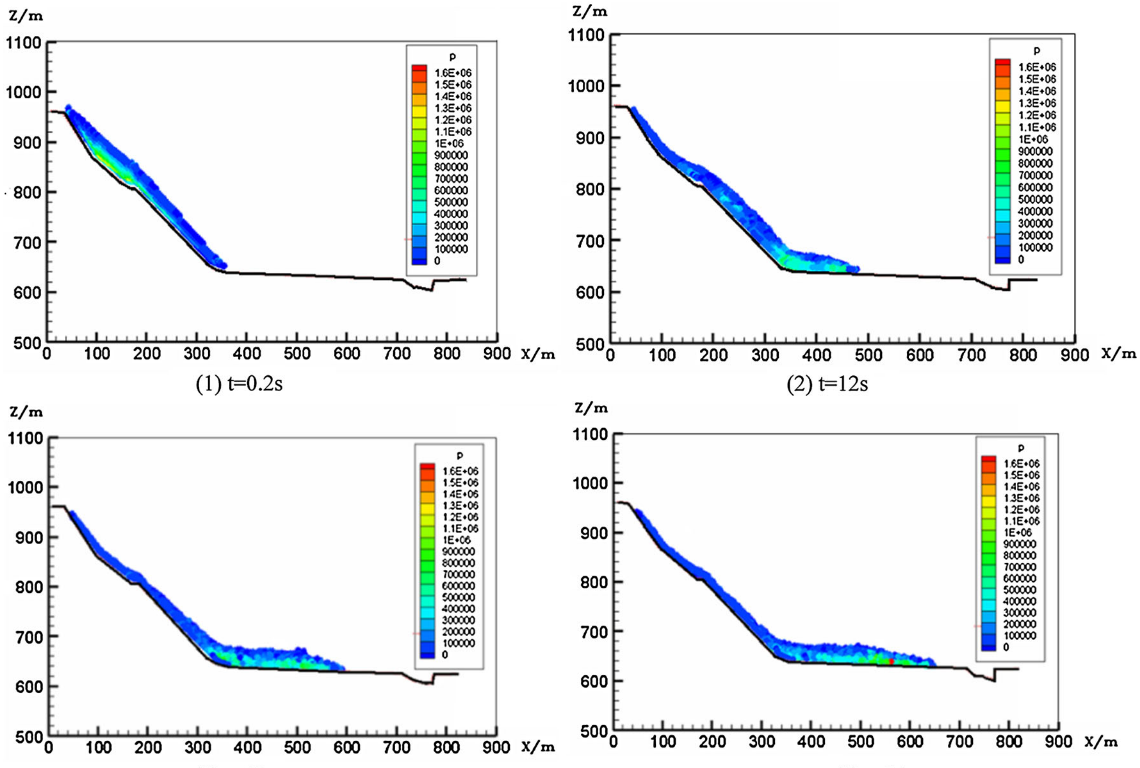

(1) t=0.2s
(2) t=12s
(3) t=18s
(4) t=24s

Fig. 6 Simulated run-out process of Wangjiayan landslide by 3D SPH model view of the SPH particle model captured in some moment of the moving process. The parameters shown in Table 3 used in the simulation were derived from triaxial tests by Huang et al. (2012). A run-out analysis was carried out to capture the whole flow process of the Donghekou landslide. Figure 8 presents the simulated run-out process of the Donghekou landslide.

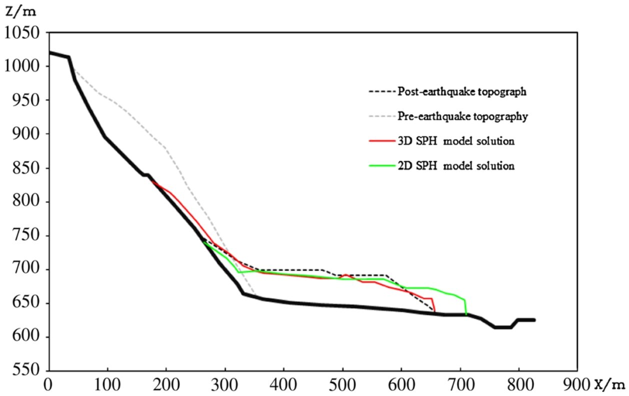

Fig. 7 Pre- and post-earthquake topographies, comparison of 2D and 3D SPH model for Wangjiayan landslide (Huang et al. 2012)

Table 3 Parameters in the run-out analysis of the Donghekou landslide (Huang et al. 2012)

Density	ρ (kg/m^3)	2,010
Equivalent viscosity coefficient	η (Pa s)	2.0
Cohesion	c (kPa)	20.5
Angle of internal friction	φ (°)	39.0

A comparison of 2D SPH simulated geometry and landslide configuration (Huang et al. 2012), and the comparison between 2D profile SPH simulation and 3D profile SPH simulation are shown in Fig. 9 in order to check the quality of 3D SPH analysis.

Analysis of simulation results

From the comparisons of 3D SPH results, 2D SPH results and surveyed landslide configurations for the Tangjiashan, Wangjiayan and Donghekou landslides, it is noticed that 3D SPH simulated geometries are similar to the surveyed landslide configurations after earthquake. It has been verified by the high degree of similarity in the situation of 2D plane. However, there are some difference between the 3D results and 2D results.

1. During the whole run-out process of the movement, the time cost in the 3D situation is longer than which in the 2D situation. For Tangjiashan landslide, it takes 80 s for the landslide from starting movement to complete the failing down of the main sliding mass in 3D SPH

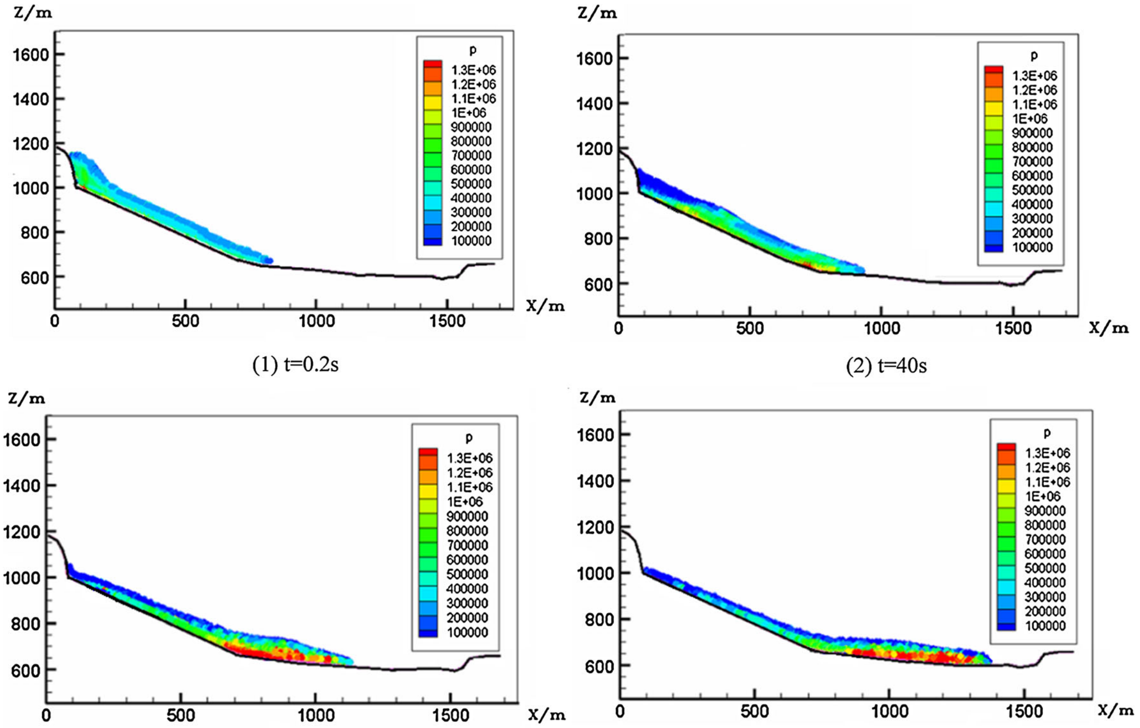

(1) t=0.2s

(2) t=40s

(3) t=80s

(4) t=116s

Fig. 8 Simulated run-out process of Donghekou landslide by 3D SPH model

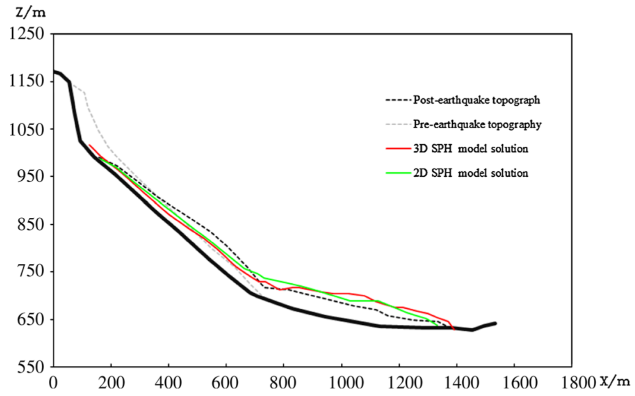

Fig. 9 Pre- and post-earthquake topographies, comparison of 2D and 3D SPH model for Donghekou landslide (Huang et al. 2012)

simulation, while it only takes 24 s in 2D SPH simulation.

2. The main sliding mass tend to hold a longer "tails" in 3D SPH simulation than that in 2D simulation. This is reasonable as 3D SPH model needs more time to complete the sliding process.
3. As 3D SPH model needs more time to complete the sliding process and the main sliding mass tends to hold a longer "tails", the modeled fluid in flow-like landslide is more viscous than that in 2D SPH model.

Although there are some differences in the flowing characteristics between the 3D SPH results and the field topographies, it indicates in some degree that 3D SPH simulations can generally reproduce the whole flow processes of typical flow-like landslides. Compared with the 2D model, the 3D model is more similar and realistic in the conditions of the natural 3D landslides. Although it can be seen that a layer of sliding mass particles "hang" on the surface (or solid wall) particles, the 3D SPH model corresponds much better to the field topographies in the slip mass part. Obviously, the 3D SPH is more reasonable. Also, it should be noted that owing to lack of experimental calibration of parameters for the SPH model in these cases, the numerical results have some errors which decrease the accuracy of the run-out analysis of these landslides.

Theoretically, the SPH numerical model proposed is able to simulate the flow-like landslides constituted of geomaterials. The fundamental and general dynamic behaviors can be derived from the SPH analysis in the run-out analysis of flow-like landslides. According to these dynamic behaviors, hazardous area predictions and hazard assessments can be put into practice and help decision makers to improve the disaster prevention. However, in practical level, it was almost impossible to know the slip surfaces of the most potential landslides, and record specific dynamic behaviors of these landslides occurred in the

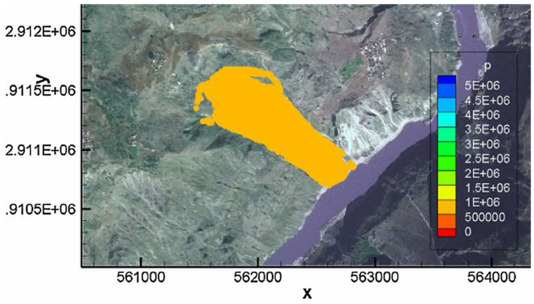

(1) t=0.05s

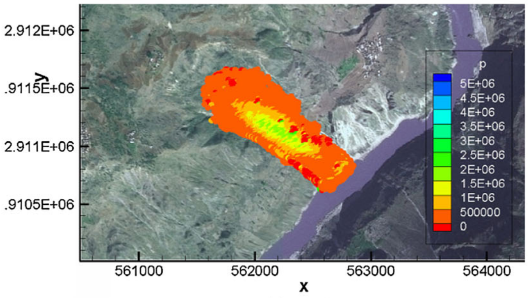

(2) t=10s

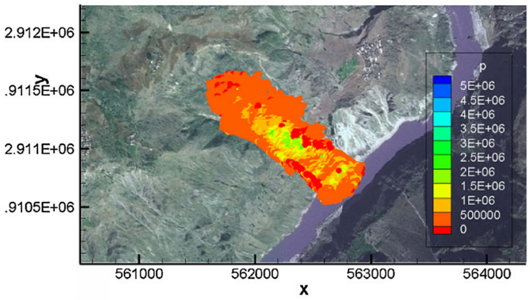

(3) t=15s

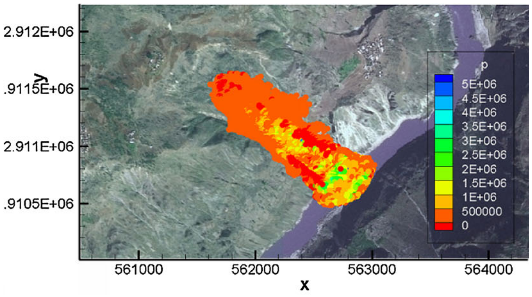

(4) t=20s

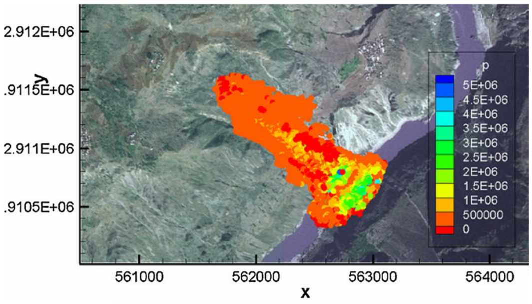

(5) t=25s

Fig. 10 Run-out prediction of Jinpingzi landslide mountainous valleys. As a result, the validation of the accuracy for the SPH simulations of flow-like landslides is mainly based on comparisons of pre-failure terrain and post-failure terrain data. But the method and the SPH simulations are sufficient for preliminary run-out analysis and assistant in hazard assessments.

Hazard area prediction of Jinpingzi landslide

Jinpingzi landslide is located on the right bank of the downstream of Wudongde cascade reach of Jinshajiang River, Yunnan Province, Southeast China. According to the traditional monitoring data, this landslide moves down slope with a rate of about 30 cm per year, which may endanger the safe construction and operation of Wudongde hydropower station. If there is an earthquake or extremely heavy rain, it is likely to induce a flow-like landslide. The terrain in Jinpingzi landslide area is shown in Supplementary figure 9. Supplementary figure 10 is an aerial photograph for Jinpingzi landslide and a photograph of the front toe.

According to the principle and method of SPH, the 3D SPH model of Jinpingzi landslide can be built to predict the hazardous area. Considering the similar geotechnical condition to Tangjiashan landslide, the parameters used in this case are the same as that used in Tangjiashan landslide. The simulated run-out process is shown in Fig. 10.

From the run-out prediction of Jinpingzi landslide, if the landslide falls down, the run-out distance may be around 400 m. It may probably block the Jinshajiang River with a rock and soil mass which is 800 m in width.

Conclusion

The flow-like landslides and other flow-like geological hazards, such as debris flows or mud flows, can cause great damages and casualties. The investigation and study on movement characteristics and mechanisms of flow-like landslides are significant and helpful to reduce the damages and casualties caused by this kind of geologic disasters.

Based on the SPH method, this paper investigates the flow-like landslides with 2D and 3D run-out analyses. The meshfree, Lagrangian particle nature makes the SPH method attractive in modeling flow-like landslides. In the SPH method, the Bingham flow model is introduced to simulate the fluid behavior of the flow-like landslides. The coefficient of equivalent viscosity is used to describe the relationship between corresponding Bingham and Newtonian flow models. The 3D SPH run-out analyses of the Tangjiashan, Wangjiayan and Donghekou landslides were applied to validate the accuracy of the model. The topographies after failure were compared with that obtained from field collected data and good agreement was found between simulation result and field data. The obtained numerical results clearly demonstrate that the SPH model can effectively simulate flow-like landslide problems, either 2D or 3D. Because landslides are dynamic process with complex geological conditions, it is necessary to introduce more suitable material models, and to validate the SPH method and numerical results with more field observations or laboratory experiments. Also, the detailed analysis on water/soil ratio and its effects on the landslide process are to be conducted in further works.

References

Cascini L, Cuomo S, Pastor M, Sorbino G, Piciullo L (2014) SPH run-out modelling of channelised landslides of the flow type. Geomorphology 214:502–513

Chen JK, Beraun JE (2000) A generalized smoothed particle hydrodynamics method for nonlinear dynamic problems. Comput Method Appl Mech Eng 190:225–239

Colagrossi A, Landrini M (2003) Numerical simulation of interfacial flows by smoothed particle hydrodynamics. J Comput Phys 191:448–475

Dai Z, Huang Y, Cheng H, Xu Q (2014) 3D numerical modeling using smoothed particle hydrodynamics of flow-like landslide propagation triggered by the 2008 Wenchuan earthquake. Eng Geol

Duncan JM (1996) State of the art: limit equilibrium and finite-element analysis of slopes. J Geotech Eng 122:577–596

Eberhardt E, Stead D, Coggan JS (2004) Numerical analysis of initiation and progressive failure in natural rock slopes—the 1991 Randa rockslide. 41(1):69–87

Gingold RA, Monaghan JJ (1977) Smoothed particles hydrodynamics: theory and application to non-spherical stars. Mon Not R Astron Soc 181:375–389

Hadush S, Yashima A, Uzuoka R (2000) Importance of viscous fluid characteristics in liquefaction induced lateral spreading analysis. Comput Geotech 27(3):199–224

Hammouri NA, Malkawi AIH, Yamin MMA (2008) Stability analysis of slopes using the finite element method and limiting equilibrium approach. Bull Eng Geol Environ 67:471–478

Hu XW, Huang RQ, Shi YB, Lv XP, Zhu HY, Wang XR (2009) Analysis of blocking river mechanism of Tangjiashan landslide and dam-breaking mode of its barrier dam. Chin J Rock Mech Eng 28(1):181–189 (in Chinese)

Huang Y, Dai Z (2014) Large deformation and failure simulations for geo-disasters using smoothed particle hydrodynamics method. Eng Geol 168:86–97

Huang RQ, Li WL (2009) Analysis of the geo-hazards triggered by the 12 May 2008 Wenchuan Earthquake, China. Bull Eng Geol Environ 68(3):363–371

Huang Y, Dai ZL, Zhang WJ, Chen ZY (2011) Visual simulation of landslide fluidized movement based on smoothed particle hydrodynamics. Nat Hazards 59:1225–1238

Huang Y, Zhang WJ, Xu Q, Xie P (2012) Run-out analysis of flow-like landslides triggered by the Ms 8.0 2008 Wenchuan earthquake using smoothed particle hydrodynamics. Landslides 9:275–283

Liu GR, Liu MB (2003) Smoothed particle hydrodynamics: a meshfree particle method. World Scientific, Singapore. ISBN 981-238-456-1

Liu MB, Liu GR (2006) Restoring particle consistency in smoothed particle hydrodynamics. Appl Numer Math 56:19–36

Liu MB, Xie WP, Liu GR (2005) Modeling incompressible flows using a finite particle method. Appl Math Model 29:1252–1270

Liu MB, Shao JR, Chang J (2012) On the treatment of solid boundary in smoothed particle hydrodynamics. Sci China Technol Sci 55(1):244–254

Lucy LB (1977) A numerical approach to the testing of fusion process. Astron J 82:1013–1024

McDougall S, Hungr O (2004) A model for the analysis of rapid landslide motion across three-dimensional terrain. Can Geotech J 41(12):1084–1097

Morris JP, Fox PJ, Zhu Y (1997) Modeling low Reynolds number incompressible flows using SPH. J Comput Phys 136(1):214–226

Pastor M, Haddad B, Sorbino G, Cuomo S (2009) A depth-integrated, coupled SPH model for flow-like landslides and related phenomena. Int J Numer Anal Meth Geomech 33:143–172

Scavia C (1995) A method for the study of crack propagation in rock structures. Geotechnique 45(3):447–463

Shao SD, Edmond YM (2003) Incompressible SPH method for simulating Newtonian and non-Newtonian flows with a free surface. Adv Water Resour 26(7):787–800

Shao JR, Li HQ, Liu GR, Liu MB (2012) An improved SPH method for modeling liquid sloshing dynamics. Comput Struct 100:18–26

Sun P, Zhang YS, Shi JS (2009) Analysis on the dynamical process of Donghekou rapid long runout landslide-debris flow triggered by great Wenchuan earthquake. In: Proceedings of the international symposium and the 7th Asian regional conference of IAEG, Chengdu, pp 902–909

Uzuoka R, Yashima A, Kawakami T, Konrod JM (1998) Fluid dynamics based prediction of liquefaction induced lateral spreading. Comput Geotech 22(3/4):234–282

Yin YP, Wang FW, Sun P (2009) Landslide hazards triggered by the 2008 Wenchuan earthquake, Sichuan, China. Landslide 6(2):139–152